Influence of stress on hydrogen-bond formation in a halogenated phthalocyanine network

Vincent Oison, Mathieu Koudia, Mathieu Abel,* and Louis Porte

Université Paul Cézanne Aix-Marseille III, Laboratoire Matériaux et Microélectronique de Provence, UMR-CNRS 6137, Faculté des Sciences de Saint Jérôme, Case 151, 13397 Marseille Cedex 20, France

(Received 28 July 2006; revised manuscript received 22 September 2006; published 31 January 2007)

The self-assemblies of half-halogenated ($ZnPcCl_8$ and $ZnPcF_8$) and nonhalogenated zinc phthalocyanine (ZnPc) molecules on an Ag(111) surface are studied by means of a combined experimental and theoretical study. The experiments involve scanning tunneling microscopy (STM) and the theoretical study is based on the topology of electron density obtained from density-functional (DFT) calculations. STM experiments reveal different structures due to the presence or not of halogen atoms at the periphery of the molecule, but the main differences are observed comparing $ZnPcCl_8$ and $ZnPcF_8$ deposits. In the case of $ZnPcCl_8$, some faults are found periodically at the end of a ripening process that are not observed in the case of $ZnPcF_8$. DFT calculations on the corresponding 2D molecular networks show differences in the nature of the H···F and H···Cl hydrogen bonds but also differences in the equilibrium molecular lattice parameter. We demonstrate that the intermolecular interaction can be tuned by chemical substitution and that the substrate-imposed stress can have a significant influence on the molecular self-assembly.

DOI: 10.1103/PhysRevB.75.035428 PACS number(s): 68.37.Ef, 71.15.Mb, 81.07.Nb

I. INTRODUCTION

In recent years, molecular thin-film growth has received considerable attention. Specific organic molecules are used as building blocks for the fabrication of surface-supported supramolecular nanostructures using supramolecular chemistry principles.[1–4] For inorganic deposition such as metal-on-metal growth, it is well known that growth morphology results from a complex competition between the equilibrium parameters of the deposit-substrate couple (e.g., interface and surface energies, mixing enthalpy, lattice mismatch, etc.) and the growth kinetics (e.g., deposition rate, deposition energy, mobility via growth temperature, etc.). The generalization of these processes to molecular systems is not a simple task because first the molecule-substrate interaction involves almost all the electrons of the molecule (particularly those present on lowest unoccupied molecular orbital: LUMO) and the first layer of the substrate and second because molecule-molecule interactions are very complex to describe. Intermolecular interactions can be weak like van der Waals interactions or stronger as hydrogen bonding or metal-ligand interactions.[5–9] Hydrogen bonding involves not only electrostatic interactions but also overlap between the electronic clouds of the molecules, large enough to impose and compact the geometry of the molecular packing. Dispersion energy (or van der Waals interaction) is also present. It corresponds to quantum dynamical correlations between two charge distributions. The strength of the dispersion is weak and its contribution to hydrogen bonding is assumed to be limited.[10–12] The two-dimensional organization of molecules at surfaces results from a subtle balance between intermolecular and molecule-substrate interactions. The mutual influence between these interactions can be interpreted as the formation of a stress in the molecular thin film.

The large extended π-conjugated molecule zinc phthalocyanine (ZnPc) is chosen to impose a flat-lying adsorption on a low-energy close-packed substrate.[13] To favor hydrogen-bond formation between molecules, we use a molecule functionalized by halogen atoms at its periphery, as represented in Fig. 1(a). We have already shown recently how the substitution of half peripheral hydrogen atoms of the ZnPc molecule by chlorine atoms allows the formation of hydrogen bonds between adjacent molecules, leading to a significant strengthening of the molecular cohesion.[14,15]

Herein we present a joint experimental and theoretical study of the molecular packing of 2,3,9,10,16,17,23,24-octafluoro zinc phthalocyanine ($ZnPcF_8$) molecules deposited on an Ag(111) surface. Molecular arrangements are studied by scanning-tunneling microscopy (STM) at room temperature. The experimental results are rationalized thanks

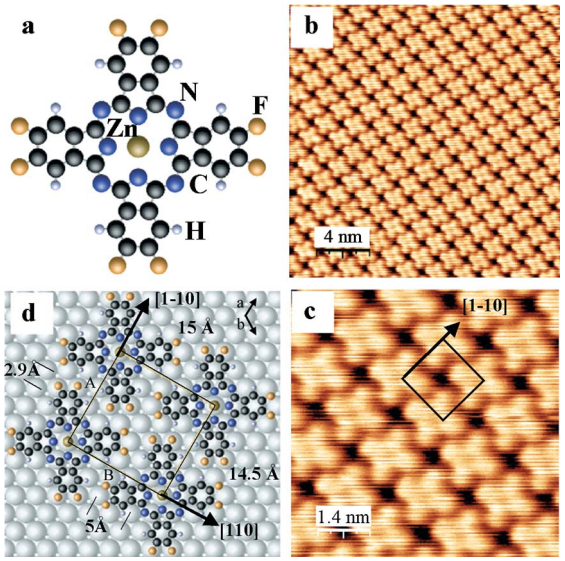

FIG. 1. (Color online) (a) Molecular structure of the $ZnPcF_8$ molecule; (b) STM image of one monolayer of $ZnPcF_8$ molecules deposited on Ag(111) at room temperature (20 nm×20 nm); (c) close-up view of the molecular self-assembly (7 nm×7 nm); (d) schematic representation of the commensurability between the molecular and the substrate networks.

to theoretical calculations based on the density functional theory (DFT). Intermolecular interactions are analyzed according to the topological approach of electron density. We show that the molecular cohesion of the $ZnPcF_8$ arrangement is due to the formation of H···F hydrogen bonds. In comparison with results obtained previously for a $ZnPcCl_8$ thin film, we show the differences between the interactions involved in the cohesion of this arrangement. This study emphasizes the influence of stress and of stress relaxation in molecular thin-film self-assemblies.

II. EXPERIMENTAL AND COMPUTATIONAL DETAILS

A. Experiments

The experiments were performed in a multicharacterization ultrahigh vacuum (UHV) chamber. The Ag(111) surface was cleaned by repeated cycles of Ar^+ sputtering and annealing (800 K). Atomically flat terraces were obtained, which were up to 200 nm in width and separated by monoatomic steps. $ZnPcF_8$ molecules were synthesized using a classical method.[16] They were then purified and deposited from a Knudsen-cell-type evaporator. During evaporation, the temperature of the molybdenum cell was maintained at 660 K, and the evaporation rate was of 0.5 ML/min. The substrate was held at 300 K. The monolayer is defined by STM measurements as 0.44 mol/nm^2, corresponding to the most compact molecular structure. STM (VT-STM Omicron) measurements were done in the constant-current mode with maximum bias voltages up to 2 V; the instrument was calibrated on atomic resolution images of different crystalline substrates. Postprocessing of the STM images was performed using the WSxM software.[17]

B. Calculations

The calculation of the molecular packing electronic structure was performed within the framework of the DFT using the generalized gradient approximation (GGA) parametrization by Perdew-Burke-Ernzerhof (PBE) for the exchange-correlation energy.[18] We used the projector-augmented wave (PAW) method,[19] in which the full wave functions and densities are expanded on a plane-wave basis set without shape approximation. The core electrons are treated within the frozen-core approximation and the band-structure calculations were carried out with a plane-wave cutoff of 40 Ry. The main difficulty is to treat molecular compounds by DFT calculations when the influence of the contribution due to the dispersion energy (or van der Waals interaction) is nonnegligible. Within the framework of traditional DFT-GGA calculations, this term—included in the exchange-correlation energy—is approximated and, consequently, poorly described. However, the GGA functional is known to be well adapted when hydrogen bonds are involved,[20] assuming static multipolar interactions (contained in the exact Hartree potential) and the electronic overlaps dominate these intermolecular contacts. In our calculations, the atomic positions are relaxed using the original fictitious Lagrangian approach of Car and Parrinello,[21] in which the atomic positions and the electronic wave functions are treated simultaneously by a set of Newton's equations.

The two-dimensional crystalline structure of $ZnPcF_8$ was studied neglecting the interactions between molecules and surface. Nevertheless, the interaction with the substrate corresponds to a charge transfer between the surface and the LUMO of the molecule, which has a small contribution on the surrounding fluorine and hydrogen atoms. Thus, we assume that the intermolecular H···F bonds should be reasonably well described. Due to the equilibrium D_{4h} symmetry of the isolated molecule, the two-dimensional (2D) molecular arrangements are simulated using a tetragonal supercell. The square base of the supercell corresponds to the 2D unit cell of the molecular thin film. The height of the tetragonal supercell was chosen large enough to ensure negligible interaction between periodic supercells along this direction. In all cases, the intramolecular geometry was not constrained and the final optimized molecular packing is found to be almost planar.

The InteGriTy software package was used for the topological analysis,[22] according to Bader's approach on the electron densities given on a three-dimensional (3D) grid.[23] One basin can be uniquely associated with one atom. It is defined as the region containing all the gradient paths terminating at the atom. The boundaries of the basin define the so-called zero-flux surface, which is never crossed by any gradient vector trajectory: $\nabla n(\mathbf{r})\cdot\mathbf{N}=\mathbf{0}$, where $\mathbf{N}$ is the normal at point $\mathbf{r}$. The charge and the dipole carried by an atom are deduced from the integration of the electron density and its first moment, respectively, over the corresponding atomic basin. A critical point (CP) corresponds to a zero value of the electron-density gradient: $\nabla n(\mathbf{r})=\mathbf{0}$. A saddle CP can be associated with each interatomic contact: at this point the electron density $n(\mathbf{r}_{CP})$ is minimum along the bond direction and maximum in the perpendicular plane. The value of $n(\mathbf{r}_{CP})$ and the value of the potential energy $V(\mathbf{r}_{CP})$ at the CP—which is deduced from the local expression of the virial theorem—are used to gauge the strength of the electronic overlap of each intermolecular bond.[23]

III. CHARACTERIZATION OF THE THIN FILM

Figure 1(b) shows a typical STM image recorded after deposition of about 1 ML of $ZnPcF_8$ molecules on Ag(111). The substrate terraces are completely covered with molecules adsorbed in a flat-lying configuration. STM observations reveal the coexistence of three molecular networks related to the three principal directions of the Ag(111) surface. The molecular network is represented by only one unit cell [Fig. 1(c)], characterized by two perpendicular vectors of approximately 15 Å each. One can notice that one of the basis vectors is aligned along the close-packed direction of the Ag(111) surface. Moreover, the two opposite arms of each molecule are aligned with the close-packed direction of the substrate. This shows the direct influence of the substrate on the orientation of the molecules, probably due to a molecule-substrate interaction stronger than a weak van der Waals interaction. This can be due to the electron-acceptor properties of phthalocyanines:[13] the interaction of phthalo-

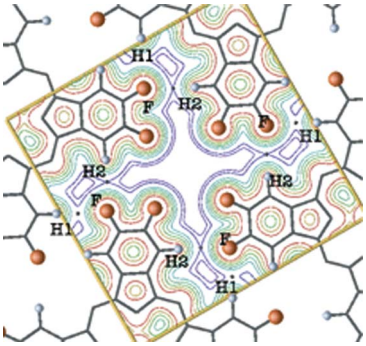

FIG. 2. (Color online) Isodensity curves in the plane of the $ZnPcF_8$ molecule: the isodensity values increase from 0.010 to $1.08e^-/Å^3$. Intermolecular H···F bond critical points are represented by tiny black spheres.

cyanines with a metallic surface results from an overlapping between the surface electronic states and the LUMO of π-symmetry. This argument should favor a site selectivity, as was demonstrated in other cases of aromatic molecular adsorption.[24,25] The observed molecular organization is rationalized by the structural model illustrated in Fig. 1(d). Each molecular lattice parameter measured by STM (15 Å) is very close to a multiple of the interatomic Ag···Ag distance along a given direction. In this model, all the molecules are positioned on equivalent adsorption sites. Thus, along the close-packed $[1\bar{1}0]$ direction, the intermolecular distance (15 Å) corresponds approximately to five interatomic Ag···Ag distances (a_{Ag}=2.9 Å):$5a_{Ag}$=14.5 Å; and, along the perpendicular [110] direction, the lattice parameter corresponds to three interatomic Ag···Ag distances ($\sqrt{3}a_{Ag}$ =5.0Å), that means $3\sqrt{3}a_{Ag}$=15Å. This indicates a possible commensurability between the molecular and substrate lattice, respectively, noted (**A**,**B**) and (**a**,**b**) in Fig. 1(d) and the unit cell can be described by the matrix **M**,

$$\begin{pmatrix} \mathbf{A} \\ \mathbf{B} \end{pmatrix} = \mathbf{M} \cdot \begin{pmatrix} \mathbf{a} \\ \mathbf{b} \end{pmatrix} \quad \text{with } \mathbf{M} = \begin{pmatrix} 5 & 0 \\ 3 & 6 \end{pmatrix}.$$

Figure 2 shows the calculated electronic structure of the $ZnPcF_8$ arrangement in the plane of molecules. It reveals the interactions between fluorine and hydrogen atoms of neighboring molecules. There are eight H···F bonds per molecule involving half of the fluorine atoms and all the hydrogen atoms. The equilibrium lattice parameter is found to be 14.6 Å and the cohesive energy 18.5 kJ mol^{-1}. The characteristics of the corresponding bond critical points (CPs) are reported in Table I. We can distinguish four short H1···F bonds and four long H2···F bonds per molecule: the corresponding bond lengths are 2.81 and 2.86 Å, respectively. In addition, the atomic charges and dipoles deduced from the integration over atomic basins reveal the electrostatic nature of the H···F bonding. Figure 3 summarizes the atomic charges and dipoles of the two-dimensional molecular network. The negative charge carried by the fluorine atoms is large and amounts to $0.64e^-$ and the hydrogen atoms carry a weak positive charge of $0.06e^-$ or $0.07e^-$. Moreover the alignment of the atomic dipoles is favorable and amounts to

TABLE I. Topological characteristics of the intermolecular H···F contacts in the $ZnPcF_8$ arrangement. The bond lengths d, electron density $n(\mathbf{r}_{CP})$, and potential energy $V(\mathbf{r}_{CP})$ are expressed at the critical points (CP) H1···F and H2···F. Atomic-point charges q and dipoles μ are obtained from the integration of $n(\mathbf{r})$ and its first moment over the atomic basins.

	H1···F	H2···F
d(Å)	2.81	2.86
$n(\mathbf{r}_{CP})(e^-/Å^3)$	0.022	0.017
$V(\mathbf{r}_{CP})$(kJ mol^{-1})	−3.70	−2.79
$q_H(e^-)$	+0.07	+0.06
$q_F(e^-)$	−0.64	−0.64
$\lvert\mu_H\rvert(e^-$ Å)	0.053	0.053
$\lvert\mu_F\rvert(e^-$ Å)	0.154	0.154

$0.154e^-$ Å and $0.053e^-$ Å for the fluorine and hydrogen atoms, respectively. Thus, these intermolecular interactions can be classified as weak hydrogen bonds because they involve not only electrostatic interactions but also an overlap between electronic clouds of molecules.

IV. DISCUSSION

A. Influence of halogen atoms

The comparison of the close-packed molecular arrangement of $ZnPcF_8$ with those of $ZnPcCl_8$ and ZnPc on Ag(111) makes it possible to analyze the role of halogen atoms X (X=Cl or F) on the intermolecular bonding mechanism.[14,15] Due to the formation of H···X interactions, the substitution of hydrogen atoms by halogen atoms at the periphery of the ZnPc molecule modifies the molecular self-assembly. The cohesive energy of the optimized molecular network is reinforced in the self-assemblies of $ZnPcF_8$ and $ZnPcCl_8$ (with-

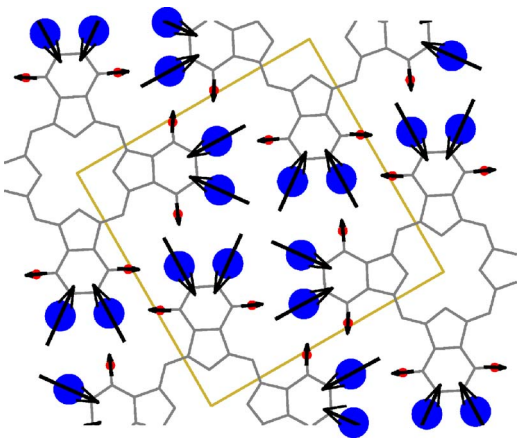

FIG. 3. (Color online) Representation of the atomic charges localized on the H and F atoms: the disk areas are proportional to the value of the charge: $+0.06e^-$ and $-0.64e^-$, respectively. Atomic dipoles are also reported: the length of the vectors is proportional to the norm of the dipoles ($0.154e^-$ Å and $0.053e^-$ Å for fluorine and hydrogen atoms, respectively).

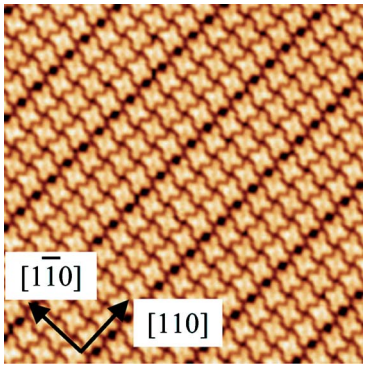

FIG. 4. (Color online) STM image of one monolayer of $ZnPcCl_8$ molecules deposited on Ag(111) at room temperature (20 nm $\times$20 nm).

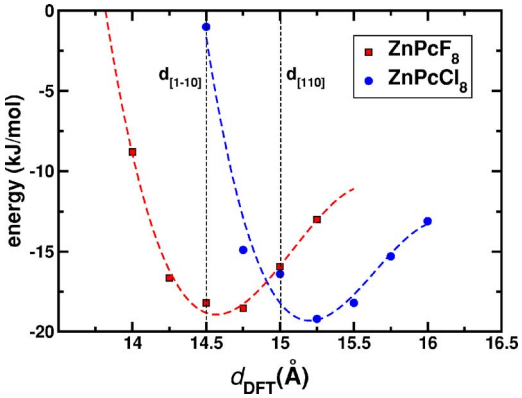

FIG. 5. (Color online) Intermolecular cohesive energy (in kJ mol^{-1}) of the close-packed arrangements of $ZnPcCl_8$ and $ZnPcF_8$ as a function of the length of the lattice parameter d_{DFT}. Squares and circles correspond to the *ab initio* results obtained for $ZnPcF_8$ and $ZnPcCl_8$ arrangements, respectively, and dotted curves to the corresponding third-order fittings. $d[110]$ and $d[1\bar{1}0]$ are, respectively, the distances between equivalent sites on the Ag(111) surface in the [110] and [1$\bar{1}$0] directions in the range of the molecular lattice.

out defect lines) molecules, which are 18.5 kJ mol^{-1} and 19.3 kJ mol^{-1}, respectively. Although $ZnPcCl_8$ and $ZnPcF_8$ have comparable cohesive energies, the nature of the H···X interactions involved in their cohesion is different. The value of the electron density and potential energy at the H···F bond CP in $ZnPcF_8$ are lower than those of the H···Cl bond CP in $ZnPcCl_8$ obtained from Ref. 14, that are 0.064 and 0.048e^-/Å^3, respectively. This shows that the H···F bonding is less covalent than the H···Cl bonding. In addition, the atomic charges and dipoles deduced from the integration over the atomic basins reveal the electrostatic nature of the H···F bonding. The negative charge carried by the fluorine atoms is three times higher than the charge carried by the chlorine atoms: 0.64e^- instead of 0.18e^-. The positive charge carried by the H atoms is also slightly higher in the $ZnPcF_8$ arrangement.

These differences in H···F and H···Cl hydrogen bonding seem to be responsible for the ripening process observed for $ZnPcCl_8$, which is not present in the case of $ZnPcF_8$. For $ZnPcCl_8$ the two-dimensional structure undergoes an evolution at room temperature, from a low-density phase resulting from weak van der Waals Cl···Cl interactions to a more compact phase induced by the activation in two steps of a H···Cl bond network.[14] For $ZnPcF_8$ molecules, only the compact arrangement is observed. In fact, due to the large negative charges carried by fluorine atoms, the electrostatic repulsion should prevent the formation of a metastable phase resulting from weak F···F van der Waals interactions. This is in agreement with the previous depositions of $CuPcCl_{16}$ on HOPG and $CoPcF_{16}$ on Au(111).[26,27] A self-assembly is observed in the case of the fully chlorinated $CuPcCl_{16}$, whereas the fully fluorinated $CoPcF_{16}$molecules cannot self-assemble due to the electrostatic repulsion between fluorine atoms.

B. Influence of stress on the molecular network

The main difference between the equilibrium self-assemblies of $ZnPcCl_8$ and $ZnPcF_8$ is the formation in the case of $ZnPcCl_8$ of a regular striped structure (represented in Fig. 4), which is not observed in the case of $ZnPcF_8$. In these two molecules, the strength of intermolecular interactions is very similar (Fig. 5), whereas the length of the equilibrium parameters is different. We will then discuss the formation of faults in terms of commensurability between the molecular and the Ag(111) networks. Table II summarizes the two-dimensional molecular lattice parameters (d_{DFT}) obtained from DFT calculations and the distance (d_{Ag}) between equivalent adsorption sites of the Ag(111) substrate in the direction of the molecular lattice parameters. The distance d_{Ag} corresponds to 5 and 3 interatomic Ag···Ag distances along the [1$\bar{1}$0] and [110] directions: 14.5 and 15 Å, respectively. Figure 5 shows the variation of the cohesive energy

TABLE II. Summary of the lattice parameters for the $ZnPcF_8$ and $ZnPcCl_8$ molecular two-dimensional structures. d_{DFT} is the length of the lattice parameters obtained from Fig. 5. d_{Ag} is the distance between equivalent adsorption sites in the lattice-parameter range deduced from STM images Fig. 1 and ϵ is the lattice mismatch.

	d_{DFT} (Å)	Direction	d_{Ag} (Å)	ϵ
$ZnPcF_8$	14.6	[1$\bar{1}$0]	14.5	−0.007
		[110]	15.0	0.027
$ZnPcCl_8$	15.3	[1$\bar{1}$0]	14.5	−0.052
		[110]	15.0	−0.02

with respect to the length of the square-lattice parameter d_{DFT}.

The equilibrium length of d_{DFT} is shorter in the case of $ZnPcF_8$: 14.6 Å instead of 15.3 Å for $ZnPcCl_8$. The difference (0.7 Å) is related to the C-F bond length, which is quite shorter than the C-Cl bond length: 1.35 Å instead of 1.75 Å. As in the case of inorganic heteroepitaxy, a lattice mismatch ϵ between molecular and substrate networks can be defined,

$$\epsilon = \frac{d_{Ag} - d_{DFT}}{d_{DFT}}. \quad (1)$$

For the $ZnPcF_8$ network, the lattice mismatch is very weak (−0.7%) along the $[1\bar{1}0]$ direction. Along the [110] direction, the mismatch is equal to 2.7% and corresponds to a dilatation of d_{DFT} of 0.3 Å. As shown in Fig. 5, such a dilatation is responsible for an energy loss less than 3 kJ mol^{-1} when dilating both the lattice parameters (e.g., less than 1.5 kJ mol^{-1} when dilating only one lattice parameter). Thus, the commensurability with the substrate is possible and implies that H···F bonds are slightly elongated along the [110] direction.

In the case of $ZnPcCl_8$, the equilibrium length of d_{DFT} is longer (15.3 Å) and consequently, the lattice mismatch ϵ becomes larger. Along the [110] direction, ϵ reaches −2%: thus, the commensurability with the substrate induces a contraction of d_{DFT} leading to an energy loss of 3 kJ mol^{-1}. Along the perpendicular $[1\bar{1}0]$ direction, the lattice mismatch (−5.2%) becomes very large: in fact the commensurability with the substrate would lead to a contraction of d_{DFT} of 0.8 Å and a destabilization of the molecular packing, as shown in Fig. 5. Hence, the $ZnPcCl_8$ molecules should move away from their equilibrium adsorption sites in order to relax the hydrogen bonds along the $[1\bar{1}0]$ direction. Every three molecular rows, the energy gain due to this relaxation would not be large anymore to counterbalance the energy loss due to the molecular displacement: thus molecules jump to the next adsorption site located at d_{Ag}=17.5 Å, leading to the formation of regular lines of faults in the $ZnPcCl_8$ self-assembly as shown in Fig. 4.

V. CONCLUSION

Combining scanning-tunneling microscopy and DFT calculations, we compare the adsorption of half-halogenated ($ZnPcCl_8$ and $ZnPcF_8$) and nonhalogenated (ZnPc) molecules on an Ag(111) substrate. First, we show that the molecules are adsorbed in a flat-lying configuration so that intermolecular interactions are governed by the peripheral atoms. In the case of the nonhalogenated ZnPc molecule,[15] the interactions between molecules can be considered as weak van der Waals interactions. The geometry of the arrangement is commensurable with the substrate network and the molecules are adsorbed on equivalent sites. The only constraint results from the distance between two adjacent adsorption sites, which must be long enough to limit steric effects between molecules. In the case of the half-halogenated $ZnPcCl_8$ and $ZnPcF_8$ molecular arrangements, the intermolecular interactions are dominated by hydrogen bonds between hydrogen and halogen atoms.[14] These interactions, which induce a massive strengthening of the cohesive energy of the molecular arrangement, are large enough to impose a compact packing. Although the final $ZnPcCl_8$ and $ZnPcF_8$ arrangements have a similar cohesive energy, the nature of the hydrogen bonding involved in the cohesion of the arrangement is different. Indeed, due to the strong polarization of the C-F bonds, the H···F bonding is more electrostatic whereas the H···Cl bonding involves a greater overlap between atoms. In the case of $ZnPcF_8$, the symmetry of the substrate matches the equilibrium molecular unit cell obtained from DFT calculation. Thus, molecules are adsorbed on equilibrium adsorption sites without constraining the H···F bond network. In the case of $ZnPcCl_8$, the substrate does not match exactly the equilibrium molecular unit cell. Thus, the periodical faults observed from STM are attributed to the relaxation of the hydrogen-bond network along the $[1\bar{1}0]$ direction. Thus we conclude that the substitution of surrounding hydrogen atoms by halogen atoms make possible to tune the intermolecular interactions by the formation of different hydrogen bonds between neighboring molecules and these hydrogen bonds can control the lattice mismatch between molecules and substrate leading to the formation of original nanostructures by stress relaxation.

ACKNOWLEDGMENTS

The authors thank M. Mossoyan and J.C. Mossoyan for synthesizing the $ZnPcF_8$, $ZnPcCl_8$, and ZnPc molecules and D. Catalin for technical support. They are also grateful to C. Katan for helpful discussion and to P.E. Blöchl for sharing his PAW code. Calculations were supported by the "Centre Informatique National de l'Enseignement Supérieur" (CINES France).

*Electronic address: mathieu.abel@univ-cezanne.fr

[1] J. M. Lehn, Science **260**, 1762 (1993).
[2] N. Bowden, A. Terfort, J. Carbeck, and G. M. Whitesides, Science **276**, 233 (1997).
[3] C. Joachim, J. K. Gimzewski, and A. Aviram, Nature (London) **408**, 541 (2000).
[4] D. Philip and J. F. Stoddart, Angew. Chem., Int. Ed. **35**, 1155 (1996).
[5] M. Abel, A. Dmitriev, R. Fasel, N. Lin, J. V. Bharth, and K. Kern, Phys. Rev. B **67**, 245407 (2003).
[6] J. A. Theobald, N. S. Oxtoby, M. A. Philips, N. R. Champness, and P. H. Beton, Nature (London) **424**, 1029 (2003).
[7] P. Messina, A. Dmitriev, N. Lin, H. Spillmann, M. Abel, J. V. Barth, and K. Kern, J. Am. Chem. Soc. **124**, 14000 (2002).
[8] J. V. Barth, J. Weckesser, N. Lin, A. Dmitriev, and K. Kern, Appl. Phys. A **76**, 645 (2003).

[9] A. Dmitriev, N. Lin, J. Weckesser, J. V. Barth, and K. Kern, J. Phys. Chem. B **106**, 6907 (2002).
[10] A. J. Stone, *The Theory of Intermolecular Forces*, The International Series of Monographs on Chemistry (Oxford University Press, 1996).
[11] G. Jeffrey, *An Introduction to Hydrogen Bonding* (Oxford University Press, Oxford, 1997).
[12] S. Scheiner, *Hydrogen Bonding. A Theoretical Perspective* (Oxford University Press, Oxford, 1997).
[13] C. Leznoff and A. Lever, *Phthalocyanines, Properties and Applications* (VCH publishers Inc., New York, 1989), Vol. 1, Chap. 1, p. 6.
[14] M. Abel, V. Oison, M. Koudia, C. Maurel, C. Katan, and L. Porte, ChemPhysChem **7**, 82 (2006).
[15] M. Koudia, M. Abel, C. Maurel, A. Bliek, D. Catalin, M. Mossoyan, J. C. Mossoyan, and L. Porte, J. Phys. Chem. B **110**,10058 (2006).
[16] K. Bayo, J. C. Mossoyan, and G. V. Ouedraogo, Spectrochim. Acta, Part A **60**, 653 (2004).
[17] WSxM, Nanotech Electronic (http://www.nanotech.es).
[18] J. P. Perdew, K. Burke, and M. Ernzerhof, Phys. Rev. Lett. **77**, 3865 (1996).
[19] P. E. Blöchl, Phys. Rev. B **50**, 17953 (1994).
[20] E. Nusterer, P. E. Blöchl, and K. Schwarz, Chem. Phys. Lett. **253**, 448 (1996).
[21] R. Car and M. Parrinello, Phys. Rev. Lett. **55**, 2471 (1985).
[22] C. Katan, P. Rabiller, C. Lecomte, M. Guezo, V. Oison, and M. Souhassou, J. Appl. Crystallogr. **36**, 65 (2003).
[23] R. F. W. Bader, *Atoms in Molecules: A Quantum Theory*, The International Series of Monographs on Chemistry (Clarendon Press, Oxford, 1990).
[24] A. Alkauskas, A. Baratoff, and C. Bruder, Phys. Rev. B **73**, 165408 (2006).
[25] E. Umbach, K. Glöckler, and M. Sokolowski, Surf. Sci. **402-404**, 20 (1998).
[26] S. Irie, A. Hoshino, K. Kuwamoto, S. Isoda, M. Miles, and T. Kobayashi, Appl. Surf. Sci. **114**, 310 (1997).
[27] L. Scudiero, K. Hipps, and D. Barlow, J. Phys. Chem. B **107**, 2903 (2003).